Fabrication and Performance of a Perovskite Solar Cell: Effect of Acetylacetone on Compact TiO₂ Layer

Busra KAYA* (iD) , Mehtap SAFAK BOROGLU (iD) , Ismail BOZ (iD)

Istanbul University-Cerrahpaşa, Departmant of Chemical Engineering, 34320, Istanbul, Turkey

Highlights
• This paper focuses on the effect of the compact TiO₂ layer on perovskite solar cells.
• $C_{12}H_{32}O_4Ti$-$C_5H_8O_2$ and $C_{16}H_{36}O_4Ti$-HNO_3 were used to synthesize c-TiO₂.
• Crack-free TiO₂ films were synthesized using acetylacetone.

Abstract

Solar energy has been the most emphasized issue in recent years, as it is sustainable and causes zero emissions. In the solar cell industry, new manufacturing protocols have led to the development of materials with enhanced properties. Over the past decades, perovskite solar cells (PSC) have obtained a power conversion efficiency (PCE) to be 25% due to the development of synthesis techniques, electrode materials, etc. There is an important relationship between the thickness of the transport layers (hole and electron) in the case of improving the yield of perovskite solar cells. We have investigated the influence of the acid-assisted and acetylacetone-assisted (AA) methods on TiO₂ films and thus the effect on the PCE of perovskite solar cells. Perovskite ($CH_3NH_3PbI_3$) layer and different compact TiO₂ (c-TiO₂) layers have been coated by the spin coating method, and the overall experimental section is made in the nitrogen medium at room temperature. Through an acid-assisted method, the cracked c-TiO₂ film was formed. The planar solar cell structure of ITO/AA-TiO₂/CH₃NH₃PbI₃/P3HT/Ag resulted in 0.03% of PCE. However, the perovskite solar cells with a mesoporous solar cell structure of ITO/ AA-TiO₂/m-TiO₂ /CH₃NH₃PbI₃/P3HT/Ag resulted in 0.1% of PCE.

1. INTRODUCTION

As a result of the population density rate, there is also a need to improve clean and sustainable energy sources. Solar cells can contribute to humanity by providing access to affordable, high-quality energy. Solar cells are a major source of renewable energy and their manufacture or research is paramount. There are three main generations of solar cells: 1- Based on silicon (monocrystalline and polycrystalline), 2- Thin film solar cells (CdTe, CIGS) and 3- Emerging solar cells (Dye-sensitized, organic, perovskite etc.) [1]. Perovskites are crystalline materials that belong to the class of semiconductors. They contain one or more types of organic and inorganic cations and halogen anions (e.g., $CH_3NH_3^+$, Pb_2^+, Cl^- or I^- etc.) that are organized into a single structure through coordination bonds. The perovskites have a perovskite structure in which the cations and anions are arranged in a cubic crystal lattice. In addition, PSC exhibits 1. over-speed charge generation, 2. higher carrier mobility, 3. favourable band gap, 4. fallen exciton binding energies and 5. slower recombination rates than other solar cell structures. Thus, it is likely that perovskites will take a prominent place in future solar cells, as well as in other photovoltaic applications where a combination of high performance, stability, low cost, and easy processing are important [2]. Compared to traditional inorganic materials, the organic-inorganic PSC have exhibited the potential to be a more efficient means of converting solar radiation into electricity. The PSC is fabricated in main sandwich structures (n-i-p) and (p-i-n) that are labelled conventional and inverted, respectively. The electron transport layer, perovskite, and hole transport layer are labelled as n, i, and p, respectively [3, 4]. As a fundamental component of PSC, the electron transport layers are responsible for the extraction and transport of electrons.

---

*Corresponding author, e-mail: busra.kaya2@ogr.iuc.edu.tr

The optimum thickness of electron compact layer not only advantages extraction of electrons but also decreases pinhole. TiO_2 [5], ZnO [6]and Sn_2O [7] are commonly used as the electron transport layers. Due to its optical properties, non-toxicity, affordability, and ease of processing, TiO_2 is commonly used in the design of perovskites-based solar cells [8]. Hong et. al (2015) investigated the influence of different coating methods on a compact layer of TiO_2 film. Their study exhibited that the thinner TiO_2 films generated pinholes while the dense films caused the texture of cracks on the surface. The qualification of the morphology of compact TiO_2 layers relies on variation in film thickness. Thus, fabricating high-performance solar cells with pinhole-free and non-crack compact TiO_2 surface morphology is desirable. The device that used the dip-coating(1:13) gave PCE of 12.8%. They observed coating highly compact TiO_2 layer (non-pinholes or non-cracked) by dip-coating route as a result of SEM images [9]. In another study, by Wang et.al., the influence of the thickness changing from 20nm to 390 nm in the compact layer on the device performance of PSC was explored. The TiO_2 compact layers were prepared by mixing acetylacetone with Ti(IV) isopropoxide solution and were coated on fluorine tin oxide (abbreviated as FTO) by spray pyrolysis. The PCE values were calculated as 1.65%, 3.17%, 2.87%, and 1.93% for 20nm, 90nm, 180nm, and 380nm respectively [10]. The compact layer thickness of the spray pyrolysis method was obtained as thinner than the compact layer thickness of the spin-coated method. Hence, the spray pyrolysis method gave higher PCE% than their spin-coated method. There are, however, still some issues with cracking and pinholes based on the film-thickness of the TiO_2 compact layer [9,11].

This work focuses on the effect of TiO_2 compact layer synthesis methods for perovskite solar cells. The TiO_2 compact layers were synthesized by the acid-assisted method and the acetylacetone-assisted method. More specifically, it demonstrates how to enhance the PCE% of perovskite solar cells by changing the TiO_2 compact layer. The perovskite ($CH_3NH_3PbI_3$), and P_3HT Ag were coated as an absorbing layer, hole transport layer, and counter electrode, respectively.

2. MATERIAL AND METHOD

We purchased, Dimethylformamide (≥99), Dimethyl sulfoxide (%99,9), ethyl alcohol(%99), lead(II) clorür (≥99), nitric acid (%65) titanium butoxide (%99), titanium isopropoxide(%97), Titanium oxide paste, poly (3-hexylthiophene-2,5-diy (≥99) from Sigma Aldrich, acetylacetone (%99) was purchase from Merck and methylammonium iodide was purchase from Dyseol.

2.1. Cleaning Procedure of ITO Glasses

Firstly, indium tin oxide (abbreviated as ITO) glasses utilized dimensions of 1.5 cm *1.5 cm. For the etching process, HCl: H_2SO_4:H_2O was mixed and then 1/3 of parts of the ITO glasses were kept in this solution for 40 min. After the etching process, the ITOs were cleaned with detergent water to remove organic impurities in an ultrasonic bath for 20 min and rinsed with deionized water. Secondly, the ITOs were sonicated in an ultrasonic bath separately in C_3H_6O and C_3H_8O. Before use, the ITOs were dried with nitrogen.

2.2. Device Preparation Procedure

The process flow for acid-assisted TiO_2 was fabricated as follows:0.13 ml of HNO_3 and 0.20 ml of deionized water were taken into a beaker and stirred for 60 min at room temperature. Besides, 1.6 ml of titanium butoxide and 4.4 ml of ethyl alcohol were taken into another beaker with stirring for 60 min at room temperature. After, titanium butoxide solution was added drop by drop into HNO_3 solutions and mixed for 120 min. The solution was used for ITO substrate coating by applying the four-step spin coating method at 1000 rpm for 5 sec and at 1500 rpm for 30 sec and at 1000 rpm for 5 sec and then at 3000 rpm for 30 sec. Finally, the layer was calcined at 500 °C (with heating at 5 °C/min) for 30 min.

The process flow for acetylacetone assisted-TiO_2 was fabricated as follows: 0.1 ml of acetylacetone and 10 ml of butanol were taken into a beaker and stirred for 60 min at 25 °C. Afterwards, 0.45 ml of titanium isopropoxide was added butanol- acetylacetone mixture. The ITO substrate was coated with a prepared solution by applying the spin coating method at 1000 rpm for 5 sec and at 3000 rpm for 30 sec. Finally, the layer was calcined at 500 ° C (with heating at 5 °C/min) for 30 min [12].

The TiO$_2$ paste and anhydrous ethanol were mixed vigorously for a mesoporous TiO$_2$ solution at 25°C for 24 h. This paste mixture was applied on an ITO substrate by using the spin coating method at 1000 rpm for 5 sec and at 3000 rpm for 30 sec. Finally, the mesoporous layer was calcined at 500 °C (with heating at 5 ⁰C/min) for 30 min.

The process flow for perovskite solution was prepared as follows, 0.7 g of PbI$_2$ and 0.8 g of CH$_3$NH$_3$I (mole ratio 1:3) were mixed in 3 ml DMF: DMSO solution with the perovskite precursor solution for 12 h at 60 °C. Afterwards, the perovskite mother solution has been filtered through a 0.45µm PVDF filter and the solution colour turned from dark yellow to light yellow. The perovskite precursor solution was fabricated on an ITO substrate by the using spin coating method at 2000 rpm for 30 sec in a nitrogen medium[13]. The coated glasses were annealed for 60 minutes at 100 °C in a nitrogen medium. The perovskite film colour turned from light yellow to black after the annealing.

For the synthesis of the hole transport layer, it was mixed with P3HT and anhydrous dichlorobenzene at a concentration of 30 mg/ml. The obtained P3HT solution was fabricated onto the perovskite layer by spin-coating at 3000 rpm for 30 s. This layer was annealed at 105 °C for 60 min in a nitrogen medium. Ultimately, Ag was coated to be 100 nm on P3HT-Perovskite-TiO2-ITO glasses by thermal evaporation. The draft of the PSC of ITO/TiO$_2$/CH$_3$NH$_3$PbI$_3$/P3HT/Ag, and (right) the diagram of energy levels was exhibited in Figure 1. Furthermore, the reel images of ITO/AA-TiO$_2$/CH$_3$NH$_3$PbI$_3$/P3HT/Ag(left) and ITO/AA-TiO$_2$/m-TiO$_2$/ CH3NH3PbI$_3$/P3HT/Ag(right) was exhibited in Figure 2.
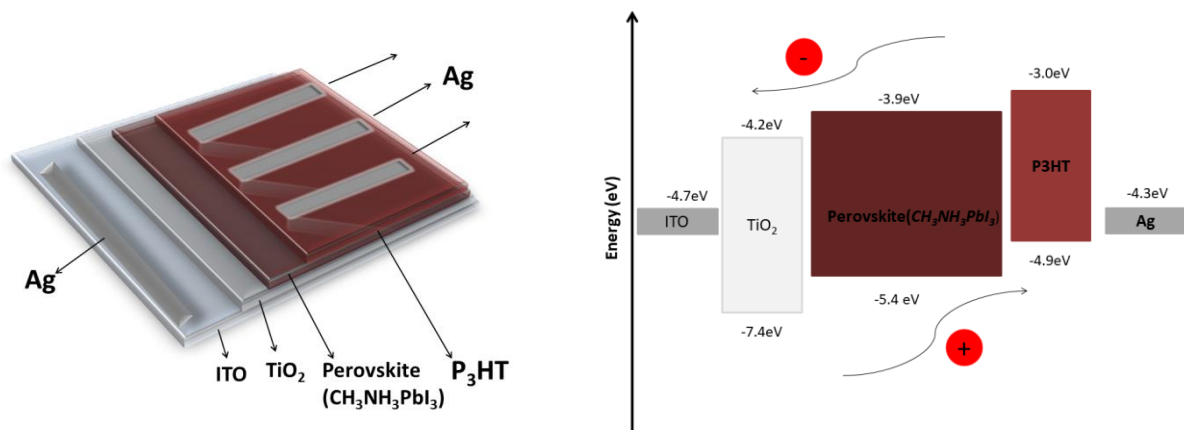
Figure 1. *Draft of the PSC of ITO/TiO$_3$/CH$_3$NH$_3$PbI$_3$/P$_3$HT/Ag, and (b) the diagram of energy levels*

Figure 2. *Illustration of the PSC of ITO/TiO$_2$/CH$_3$NH$_3$PbI$_3$/P3HT/Ag, and (b) the Reel images of ITO/AA-TiO$_2$/CH$_3$NH$_3$PbI$_3$/P3HT/Ag(left) and ITO/AA-TiO$_2$/m-TiO$_2$/ CH$_3$NH$_3$PbI$_3$/P3HT/Ag(right)*

2.3. Device Characterization

The TiO$_2$ and perovskite layers were examined from XRD using trademark Rigaku D / Max-2200 in diffracted angle from 10° to 60° and a scan speed of 2°/min with CuKα radiation (features 40 kV and 30 mA current), the wavelength of 0,15418 nm. The synthesized TiO$_2$ films were examined with a Nikon

Eclipse 2000 branded microscope at a magnification of x 50 times after calcination. The perovskite film structure was investigated by Fourier Transform Infrared Spectroscopy between a range of 400-4000 cm^{-1} at 128 accumulations per scan.

For absorbance measurement was used by trade Ocean Optics USB-4000 spectrophotometer was in the range of wavelength 200-800nm. The photovoltaic cell structure was measured with AM 1.5G 1 sun illumination, and Keithley 2401 in order to obtain characteristics of voltage-current density. The current versus current-voltage curves that complete the circuit against the sent constant voltage were created. With the help of current-voltage curves generated, short circuit current (Isc), open-circuit voltage (Voc), fill factor (FF) and power conversion efficiency data were obtained.

3. RESULTS AND DISCUSSION

3.1. Surface Survey Results of Compact TiO$_2$ Film

The surface of TiO$_2$ films was examined with a camera at 50 times magnification. As shown in Figure 3(left), for the TiO$_2$ solution synthesized by the acid-assisted-TiO$_2$ method, homogeneity could not be achieved in the film surface and cracked surface structures were detected at both 1500 rpm and 3000 rpm coating rates. However, as shown in Figure 3(right) cracked structures could not be seen in TiO$_2$ films due to using acetylacetone.
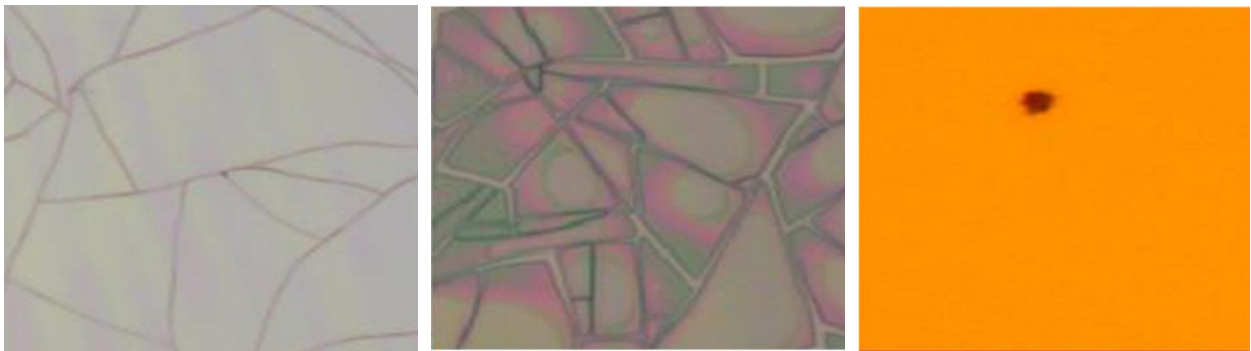
***Figure 3.** TiO$_2$ thin film synthesized acid assisted after a single coating process at 1500rpm and 3000 rpm (left), b) TiO$_2$ thin film synthesized acetylacetone using method (right)*

3.2. XRD Results of TiO$_2$ films

The XRD pattern of TiO$_2$ films on ITO glass was exhibited in Figure 4. The peaks observed at 2Ө: 35º, 37.5º were attributed to the anatase TiO$_2$ phase (JCPDS card 21-1272) [14]. The crystal sizes were calculated by the Debye Scherer equation for AA-assisted TiO$_2$ film and acid-assisted TiO$_2$ film as 14nm, and 20 nm, respectively [15]. The acid-assisted method led to the formation of a more crystalline structure.
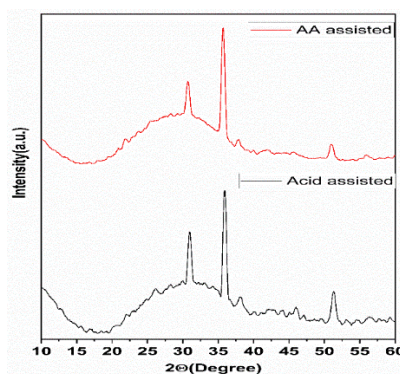
***Figure 4.** XRD patterns of different TiO$_2$ layers on ITO glass*

3.3. XRD and FTIR Results of Perovskite Thin Film

The XRD pattern of perovskite film on ITO-TiO$_2$ glass was exhibited in Figure 5A. From the figure, the diffraction peaks observed at 2Θ: 14,7º, 20.48º, 24.05º, 25.12º, 28.96º, 32.04°, 42.14° and 50.76° can be referred to as the (110), (112), (211), (202), (004), (220), (213), (224), (314) and (404) planes of tetragonal CH$_3$NH$_3$PbI$_3$, respectively[16]. Furthermore, the weak diffraction peaks detected at 28° and 35° were assigned to (200) and (213) planes of the cubic structure of CH$_3$NH$_3$PbI$_3$ [17]. The diffraction peaks of belonging PbI$_2$ at 12.70° and 39.58° were not observed due to PbI$_2$ and CH$_3$NH$_3$I completely reacting [13]. The FTIR spectra of the film of perovskite was exhibited in Figure 5B. The bonds belonging to C, H, and N were detected while the bonds belonging to Pb-I were not detected. The characteristic peaks of perovskite detected for N–H symmetrical stretch vibration at 2920 cm^{-1}, 2362 cm^{-1} asymmetrical CH$_3$ stretch vibration, N–H asymmetrical bending at 1664 cm^{-1}, C–H bending vibration at 963 cm^{-1}, CH$_3$-NH$_3^+$rock at 848 cm^{-1}. Also, a weak O-H bond peak was detected at 3600 cm^{-1} due to physical adsorption on perovskite films [2].
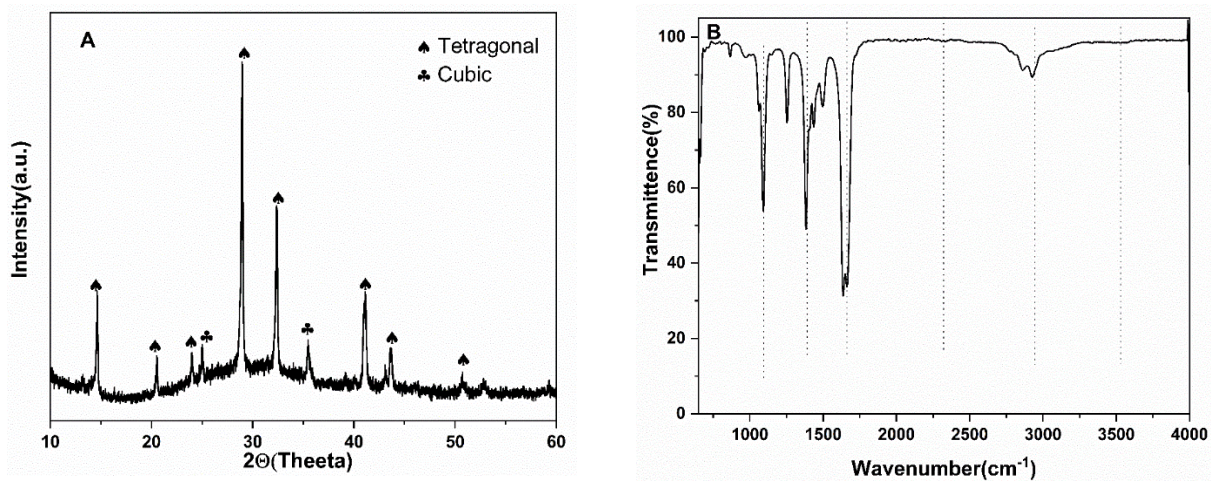

Figure 5. *XRD pattern and FTIR of a perovskite thin film on ITO glass*

### 3.4. UV-Vis Analysis Results of TiO$_2$ and Perovskite Thin Film

The absorbance graph of TiO$_2$ (compact and mesoporous) and CH$_3$NH$_3$PbI$_3$ thin films were exhibited in Figure 6. The absorbance graph of compact TiO$_2$, mesoporous TiO$_2$ and CH$_3$NH$_3$PbI$_3$ thin films were exhibited in Figure 6. A thin film of c-TiO$_2$ was found to exhibit good absorbance between 200 and 470 nanometers. In the range of 200-500 nm, the intensity of absorption increased with a mesoporous TiO$_2$ coating. Furthermore, the results demonstrate that the coated perovskite on TiO$_2$ exhibits significant absorption between 200 nm and 800 nm. Based on Runa et.al's (2018) study, quality perovskite films displayed absorbance as high as 800 nm [18].
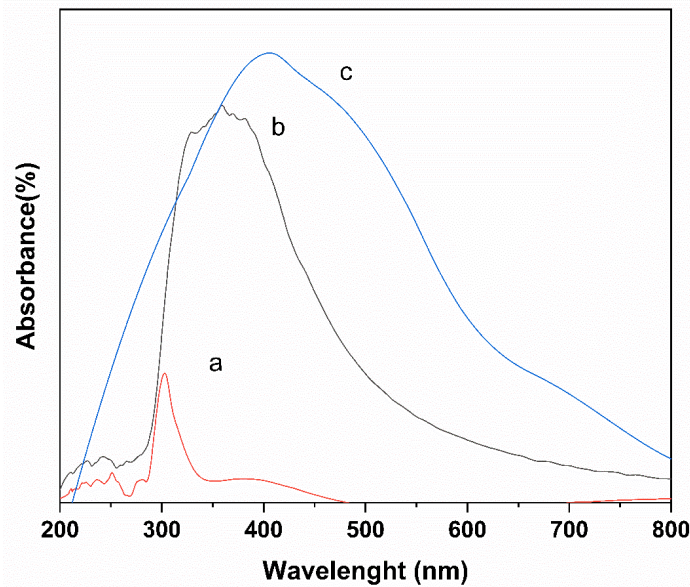
Figure 6*. The absorption spectra of different thin films a. Compact TiO₂, b. Mesoporous TiO₂ c. Perovskite thin film*

3.5. Current Voltage of Fabricated Solar Cells Investigation of Characteristics

Figure 7 exhibited the J-V curves of ITO/AA-TiO$_2$/CH$_3$NH$_3$PbI$_3$/P3HT/Ag and ITO/ AA-TiO$_2$ / m- TiO$_2$ /CH$_3$NH$_3$PbI$_3$/P3HT/Ag solar cells. The findings of Voc, Jsc, FF, and PCE were given in Table 1. The ITO/Acid-TiO$_2$ (1500 rpm and 3000 rpm)/CH$_3$NH$_3$PbI$_3$/P3HT/Ag solar cells did not give current due to a short circuit. The microscope image (Figure 3) exhibited that there was clearly no homogeneous surface structure in acid-assisted TiO$_2$. In the present study, it was seen that the surface of the c-TiO$_2$ film is an important parameter for solar cells. Titanium (IV) alkoxide was rapidly hydrolyzed in the acid-water solution and hence cracks occurred in the film structure. However, the addition of acetylacetone as a stabilizing agent to the synthesis medium acts as a nucleophilic reactant and replaces the alkoxy group[12]. Therefore, the hydrolysis rate of the Ti solution reduces, resulting in a non-cracked film structure. (Figure 3). When the current-voltage and other values of c-TiO$_2$/PSC and c-TiO$_2$/m-TiO$_2$ PSC were compared, c-TiO$_2$/m-TiO$_2$ solar cells had better performance values than c-TiO$_2$ solar cells. Due to the mesoporous TiO$_2$ films having pores, an enhancement in the contact area with the perovskite has occurred and a better PCE result has been obtained. In addition, it is thought that the m-TiO$_2$ nanoparticles help the controlled growth of perovskite crystals [19] It can be explained that with the increase in J$_{SC}$ of cTiO$_2$/m-TiO$_2$ solar cell, there is a getting better electrical conductivity, resulting in preferable charge carrier mobility with m-TiO$_2$ coating.
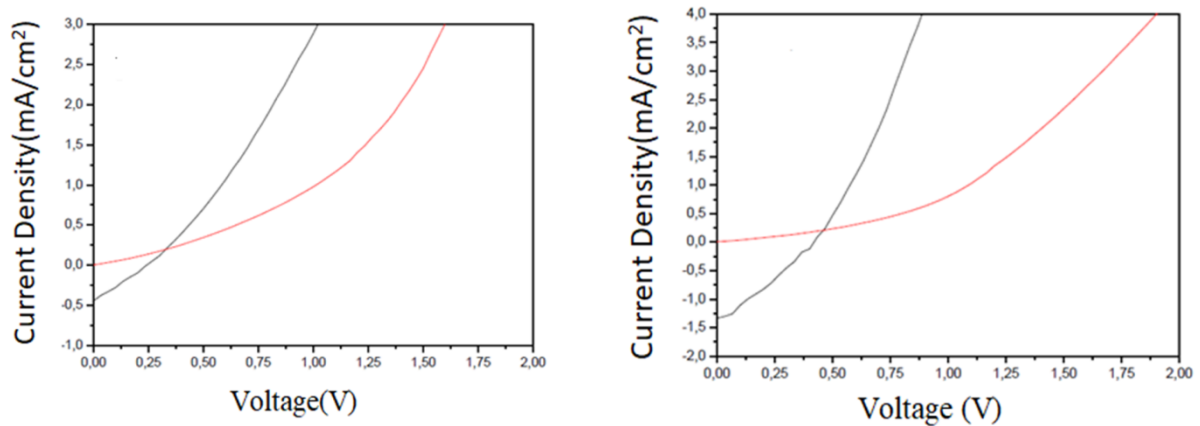
Figure 7. *Measured voltage-current density characteristics of ITO/AA-TiO$_2$ /CH$_3$NH$_3$PbI$_3$/P3HT/Ag (left) and ITO/AA-TiO$_2$/m-TiO$_2$/CH$_3$NH$_3$PbI$_3$/P3HT/Ag (right) photovoltaic cell under in the dark and illumination solar light*

Table 1. *Obtained photovoltaic results from fabricated solar cells*

No	Structure	Voc (mV)	Jsc (mA/cm^2)	FF	η(%)
1	ITO/Acid-TiO$_2$(1500 rpm)/perovskite/P3HT/Ag	nd	nd	nd	nd
2	ITO/Acid-TiO$_2$(3000 rpm)/perovskite/P3HT/Ag	nd	nd	nd	nd
3	ITO/AA-TiO$_2$/perovskite/P3HT/Ag	267	0.4	0.3	0.03
4	ITO/AA-TiO$_2$/m-TiO$_2$/perovskite/P3HT/Ag	367	0.7	0.3	0.1

nd: not detected

4. RESULTS

In our study, various c-TiO$_2$ were synthesized by acid-assisted and AA-assisted methods. The homogeneous structure could not be obtained by the acid-assisted method and cracks occurred in the film whereas a non-cracked structure could be obtained by the AA-assisted method. The obtained acid-assisted c-TiO$_2$ layer did not give any current. The cracked compact TiO$_2$ layer would not produce any current by allowing contact between the materials. The best PCE% was obtained by ITO/AA-TiO$_2$/m-TiO$_2$/perovskite/P3HT/Ag and was found to be %0.1. According to studies in the literature, the thick-coated films are believed to be the reason for the low yields. The relationship between electron transport film thickness and photovoltaic activity was studied by Cheng et. al. (2022). The electron transport films were synthesized at different solution concentrations (0.25M-1.0M) and coated on FTO. The PCE values were found as 21% >19.7%, 19.1%, and 18.3% for 0.75M, 0.5M, 1.0M, and 0.25M, respectively. A higher film thickness did not result in a greater increase in photovoltaic activity. As a result of their research, they determined the optimum film thickness as 60 nm (for 0.75M) for the highest photovoltaic activity [7]. Using a numerical simulation, Saki et. al. (2022) examined the result of the thickness of the ETL on cell productivity. Different ETLs were studied with thicknesses ranging from 100 to 1500 nm. For TiO$_2$, SnO$_2$ and ZnO, the V$_{OC}$ and FF decreased with an increase in ETL thickness. The thickness of both HTL and ETL was found to be optimum at 80 nm and thereby PCE values were obtained to be 18%, 17.1% and 16.3% for Sn$_2$O, ZnO and TiO$_2$, respectively [20]. In a similar study, Kim et. al. (2015) investigated hole transport layer thickness to improve the devices' performances. The performance efficiencies of the device varied depending on the HTL thickness (from 100nm to 700nm). The device with an HTL of 180 nm gave the highest PCE of 16% of whole devices. According to their studies, the perovskite film thickness should not be thick than 150 nm in order to maximize power conversion efficiency. These studies and presented figures indicate that electron and hole layer thickness significantly impact device performance [21].

ETL/HTL thickness values with a higher value cause charge carriers to travel a longer distance. To avoid increasing the series resistance of the devices and to ensure homogeneous perovskite coating, the thickness of the transport layers is crucial. Result of the literature studies, the thickness of transport layers should be formed between nanometers (50-100 nm).

ACKNOWLEDGEMENTS

CONFLICTS OF INTEREST

No conflict of interest was declared by the authors.

REFERENCES

[1]   Ibn-Mohammed, T., Koh, S. C. L., Reaney, I. M., Acquaye, A., Schileo, G., Mustapha, K. B., and Greenough, R., "Perovskite solar cells: An integrated hybrid lifecycle assessment and review in comparison with other photovoltaic technologies", Renewable and Sustainable Energy Reviews, 80: 1321–1344, (2017).

[2]   Pitchaiya, S., Natarajan, M., Santhanam, A., Asokan, V., Ramakrishnan, V. M., Selvaraj, Y., and Velauthapillai, D., "The Performance of $CH_3NH_3PbI_3$ - Nanoparticles based – Perovskite Solar Cells Fabricated by Facile Powder press Technique", Materials Research Bulletin, 108: 61–72, (2018).

[3]   Ojanperä, A. M. M., "Mesoscopic Perovskite Solar Cells: Efficiency Enhancement via Optimization of the Titania Anode", Master's thesis, Tampere University of Technology, Finland, 54, (2015).

[4]   Yu, Y., Gao, P., "Development of electron and hole selective contact materials for perovskite solar cells", Chinese Chemical Letters, 28: 1144–1152, (2017).

[5]   Deng, X., Wilkes, G. C., Chen, A. Z., Prasad, N. S., Gupta, M. C., and Choi, J. J., "Room-temperature processing of TiO_x electron transporting layer for perovskite solar cells", The Journal of Physical Chemistry Letters, 8: 3206-3210, (2017).

[6]   Ahmad, S., Abbas, H., Khan, M. B., Nagal, V., Hafiz, A. K., and Khan, Z. H., "ZnO for stable and efficient perovskite bulk heterojunction solar cell fabricated under ambient atmosphere", Solar Energy, 216: 164–170, (2021).

[7]   Cheng, N., Yu, Z., Li, W., Liu, Z., Lei, B., Zi, W., and Rodríguez-Gallegos, C. D., "Highly efficient perovskite solar cells employing SnO_2 electron transporting layer derived from a tin oxalate precursor solution", Journal of Power Sources, 544, (2022).

[8]   Niu, B., Wang, X., Wu, K., He, X., and Zhang, R., "Mesoporous titanium dioxide: Synthesis and applications in photocatalysis, energy and biology", Materials, 11: 1910, (2018).

[9]   Hong, S., Han, A., Lee, E.C., Ko, K.-W., Park, J.-H., Song H.-J., Han, M.-H., and Han, C.-H., "A facile and low-cost fabrication of TiO_2 compact layer for efficient perovskite solar cells", Current Applied Physics, 15: 574–579, (2015).

[10]   Wang, X., Fang, Y., He, L., Wang, Q., and Wu, T., "Influence of compact TiO2 layer on the photovoltaic characteristics of the organometal halide perovskite-based solar cells", Materials Science Semiconductor Processing, 27: 569–576, (2014).

[11] Nyongesa, F., "Electrophoretic Deposition of Titanium Dioxide Thin Films for Photocatalytic Water Purification Systems", Advances in Materials, 6: 31-37, (2017).

[12] Spiridonova, J., Katerski, A., Danilson, M., Krichevskaya, M., Krunks, M., and Oja, A., "Effect of the Titanium Isopropoxide: Acetylacetone Molar Ratio on the Photocatalytic Activity of TiO_2 Thin Films", Molecules, 24: 4326, (2019).

[13] Asad, J., Shaat, S. K. K., Musleh, H., Shurrab, N., Issa, A., Lahmar, A., and Al Dahoudi, N., "Perovskite solar cells free of hole transport layer", Journal of Sol-Gel Science and Technology, 90: 443–449, (2019).

[14] Homola, T., Pospisil, J., Shekargoftar, M., Svoboda, T., Hvojnik, M., Gemeiner, P., and Dzik, P., "Perovskite Solar Cells with Low-Cost TiO_2 Mesoporous Photoanodes Prepared by Rapid Low-Temperature (70 °C) Plasma Processing", Applied Energy Materials, 3: 12009–12018, (2020).

[15] Jourdani, R., Outzourhit, A., Oueriagli, A., Aitelhabti, D., Ameziane, E. L., Barazzouk, S., and Hotchandani, S., "Structural, optical and electrochromic properties of nanocrystalline TiO_2 thin films prepared by spin coating", Active and Passive Electronic Components, 27: 125–131, (2004).

[16] Li, S., Yang, B., Wu, R., Zhang, C., Zhang, C., Tang, X. F., and Yang, J., "High-quality $CH_3NH_3PbI_3$ thin film fabricated via intramolecular exchange for efficient planar heterojunction perovskite solar cells", Organic Electronics, 39: 304–310, (2016).

[17] Sharma, A., and Chaure, N. B., "Studies on $CH_3NH_3PbI_3$ prepared by low-cost wet chemical technique", Applied Physics A, 25: 1-7, (2019).

[18] Runa, A., Feng, S., Wen, G., Feng, F., Wang, J., Liu, L., Su, P., Yang, H., and Fu, W., "Highly reproducible perovskite solar cells based on solution coating from mixed solvents", Journal of Material Science, 53: 3590–3602, (2018).

[19] Habibi, M., Zabihi, F., Ahmadian-Yazdi, M.R., and Eslamian, M., "Progress in emerging solution-processed thin film solar cells - Part II: Perovskite solar cells", Renewable and Sustainable Energy Reviews, 62: 1012–1031, (2015).

[20] Sakib, S., Mohd Noor, M.Y., Salim, M.R., Abdullah, A.S., Azmi, A.I., M.H., and Ibrahim, M.H., "Effect of transport layer thickness in lead-based perovskite solar cell: A numerical simulation", Materials Today Processing, (2022).

[21] Kim, W., Shinde, D. V., and Park, T., "Thickness of the hole transport layer in perovskite solar cells: Performance versus reproducibility", Royal Society Chemistry Advances, 5: 99356–99360, (2015).